JOURNAL OF APPLIED ELECTROCHEMISTRY 23 (1993) 296–307

Redox chemistry of H_2S oxidation by the British Gas Stretford Process
Part III: Electrochemical behaviour of anthraquinone 2,7 disulphonate in alkaline electrolytes

G. H. KELSALL, I. THOMPSON*

Department of Mineral Resources Engineering, Imperial College, London SW7 2BP, Great Britain

Received 30 January 1991; revised 31 July 1992

Electrochemical reduction of aqueous anthraquinone 2,7 disulphonate (AQ27DS) solutions at pH 9.3 were studied at Hg, Au and Pt electrodes. Cyclic voltammograms showed about 40 mV potential separation of the single pair of current peaks, precluding a simple one or two electron process. Charge measurements in controlled potential exhaustive reductions indicated a 2 mol e^- per mol AQ27DS process leading to quinolate anions, whereas the partially reduced solution showed an EPR spectrum, indicating the presence of radical species, which, if produced directly, would involve only a 1 mol e^- per mol AQ27DS process. U.v.–visible and EPR spectra of the deep red partially reduced AQ27DS solutions showed that both radical anions ($AQ27DS^-$) and fully reduced anthraquinolate were present; $AQ27DS^-$ radicals predominated at low conversions, while complete conversion produced $AQ27DSH^-$ ions. The AQ27DS diffusion coefficient was determined as $3.73 \times 10^{-10}\,m^2\,s^{-1}$ from steady-state voltammetry at a gold rotating disc electrode.

The results are congruous with a reduction mechanism involving an initial 2 mol e^- per mol AQ27DS process to give anthraquinolate anions, from which electron transfer in solution to AQ27DS species produced $AQ27DS^-$ radical anions (a comproportionation). The comproportionation equilibrium constant was estimated as between 0.2 and 4.0 from cyclic voltammograms; together with a value of $pK_{a2}(AQ27DSH_2) = 10.8$ from the literature, this enabled the solution composition, and hence the major absorption spectral changes, to be predicted as a function of conversion. From a calculated potential–pH diagram, the AQ27DS reduction mechanism was predicted to involve disproportionation of the radical anions at pH $\ll$ 9.3 and two sequential one electron reductions at pH $\gg$ 9.3

Nomenclature

A	electrode area (m^2)
c	concentration ($mol\,m^{-3}$)
D	diffusion coefficient ($m^2\,s^{-1}$)
E^0	standard reversible electrode potential against SHE (V)
F	Faraday constant 96 485 C $(mol\,e^-)^{-1}$
HMDE	hanging mercury drop electrode (–)
i	current density ($A\,m^{-2}$)
i_L	mass transport limited current density ($A\,m^{-2}$)
i_{sp}	peak current density at HMDE ($A\,m^{-2}$)
I_K, I'_K	EPR sensitivity factors, constants for a given geometry
$\bar{k}_m$	mean mass transport rate constant ($m\,s^{-1}$)
l	length of EPR cavity (m)
n	number of moles of reactant
r	radius of the EPR tube (m)
R	gas constant (8.314 41 $J\,mol^{-1}\,K^{-1}$)
S	EPR signal strength (–)
S_0	EPR signal strength for one mole of spins within cavity (–)
t	time (s)
T	temperature (K)
V	electrolyte volume (m^3)
V_f	volumetric flow rate ($m^3\,s^{-1}$)
X_e	length of electrode (m)
z	number of moles e^- per mole of reactant (–)

Greek symbols

ε	molar absorptivity ($m^2\,mol^{-1}$)
δ	Nernst diffusion layer thickness (m)
η	kinematic viscosity ($m^2\,s^{-1}$)
ν	potential sweep rate ($V\,s^{-1}$)
ω	RDE rotation rate (s^{-1})

* Present address: Lever Development Centre Casalpusterlengo, via Lever Gibbs, 20071 Casalpusterlengo, Italy.

0021-891X

1. Introduction

1.1. *The British Gas Stretford Process*

This process [1–3] uses atmospheric oxygen to achieve the oxidation of hydrogen sulphide absorbed in aqueous solution, producing elemental sulphur and water:

$$2H_2S + 0.5O_2 \longrightarrow S + H_2O \quad (1)$$

In the absence of catalysts, this oxidation is extremely slow. Furthermore, it may produce higher oxidation state sulphur species such as thiosulphate, resulting in an effluent problem:

$$2H_2S + 2O_2 + 2OH^- \longrightarrow S_2O_3^{2-} + 3H_2O \quad (2)$$

Water soluble anthraquinone derivatives, such as anthraquinone 2,7 disulphonate (AQ27DS), have been found to be effective catalysts for the aerial oxidation of H_2S to sulphur and are thought to act via a redox cycle. Hence, the electrochemical behaviour of anthraquinone 2,7 disulphonate (AQ27DS) (Fig. 1) was investigated, as part of a study of the redox chemistry of the Stretford Process [3]. The chemistry of its other component redox systems (S/HS^- [4, 5] and V(V)/V(IV) [6, 7] is described separately.

1.2. *Redox chemistry of quinones*

The widely studied reduction of quinones has been reviewed by Chambers [8, 9]. Bailey and Ritchie [10] reported that reduction of a range of quinones (Q) in acidic aqueous solutions invariably proceeded by a 2 mol e^- (mol Q)$^{-1}$ process yielding the corresponding quinolate ($QH_2/QH^-/Q^{2-}$). Quershi *et al.* [11] found the electrochemical reduction of 18 hydroxy-anthraquinones derivatives behaved similarly:

$$AQ + 2e^- \longrightarrow AQ^{2-} \quad (3)$$

Reduction may or may not be accompanied by protonation, depending on the first and second acidity constants of the corresponding anthraquinolate reduction products [8, 9].

However, the electrochemical reduction of an anthraquinone is dependent on the stability of the corresponding semiquinones [12], as measured by the value of the comproportionation constant K_c.

$$AQ + AQ^{2-} \rightleftharpoons 2AQ^{-} \quad (4)$$

$$K_c = \frac{[AQ^-]^2}{[AQ][AQ^{2-}]} \quad (5)$$

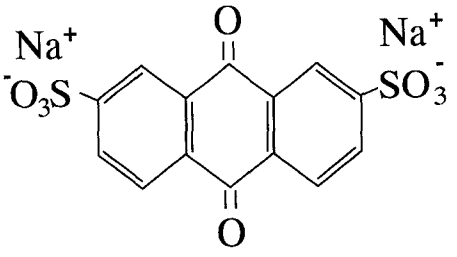

Fig. 1. Structure of (di-sodium) anthraquinone 2,7 disulphonate (AQ27DS)

The voltammetric behaviour of quinones is dependent on the kinetics of the above reaction, as well as the value of its equilibrium constant. Only if the equilibrium is established rapidly compared to the time for a potential sweep, will the value of K_c affect the reduction wave. In such cases, if $K_c \ll 1$, a single wave corresponding to a two electron reduction is observed; if $K_c \gg 16$ then two separate waves are observed, corresponding to two consecutive one electron reductions [12]. However, when K_c has a value between 1 and 16, a single wave can be observed, with a slope corresponding to anything between 2/3 and 2 electrons per molecule. This explains why, in many instances, single reduction waves can be observed, indicating electron transfer numbers close to one, while coulometry always results in a value close to 2.

Savenko *et al.* [13, 14] noted that the polarography of anthraquinone-1,5-disulphonic acid was affected by adsorption of the oxidized and reduced forms on a mercury electrode, and resulted in the inhibition of the reduction reaction, so confounding the derivation of kinetic information.

Moore [15] studied the u.v. and Raman spectra of the species generated by the irradiation of anthraquinone 2,6 disulphonate using laser light at 351 nm. The radical anion was extremely long lived in the absence of oxygen, and showed u.v. absorbances at 400 and 510 nm [15, 16]; the protonated form absorbed only at 400 nm. If oxygen was present, the radical was quenched rapidly, a process which results in the production of superoxide ions:

$$AQ26DS^- + O_2 \longrightarrow AQ26DS + O_2^- \quad (6)$$

The reaction rate was found to be extremely rapid, with a rate constant of 9×10^5 mol^{-1} m^3 s^{-1}. The product superoxide ions are powerful oxidizing agents, reacting with water to produce hydrogen peroxide [17]:

$$2O_2^- + H_2O \longrightarrow O_2 + HO_2^- + OH^- \quad (7)$$

$$HO_2^- + H_2O \rightleftharpoons H_2O_2 + OH^- \quad (8)$$

Hydrogen peroxide can also be produced by reacting oxygen with electrochemically reduced AQ26DS. Keita and Nadjo [18] reduced the water-soluble sodium salt of anthraquinone 2,6 disulphonate (Na_2AQ26DS) electrochemically:

$$AQ26DS + 2H^+ + 2e^- \longrightarrow AQ26DSH_2 \quad (9)$$

and then reoxidized it with oxygen to produce hydrogen peroxide with 100% efficiency:

$$AQ26DSH_2 + O_2 \longrightarrow AQ26DS + H_2O_2 \quad (10)$$

Therefore, it is feasible that, on re-oxidation, the reduced AQ27DS in the Stretford Process solutions generates hydrogen peroxide *in situ*; this is sufficiently powerful in alkaline solution to oxidize the sulphide in solution to sulphur and to oxidize the reduced forms of other dissolved catalysts. A process for H_2O_2 production has been patented [19, 20], involving CaO_2 precipitation from reduced AQ27DS solutions treated

with $Ca(OH)_2 + O_2$, followed by decomposition of CaO_2 with CO_2, to yield H_2O_2 with an apparent current efficiency of 95%.

The objective of the presently reported work was to define the kinetics and reaction products of AQ27DS reduction at pH 9.3, relevant to Stretford Processes, to enable its catalytic function in the process to be understood. This involved cyclic voltammetry at stationary and rotating disc electrodes, and controlled potential coulometry coupled to analysis by u.v.-visible spectrophotometry and EPR spectroscopy. However, the restricted range conditions studied, particularly with respect to the initial reactant concentration and pH, precluded a definitive mechanism being assigned.

2. Experimental details

2.1. *Purification of 2,7 anthraquinone disulphonate*

A sample of the crude di-sodium 2,7 anthraquinone disulphonate (L. B. Holliday Co. Ltd, Huddersfield, UK) was dissolved in distilled water, and purified using a column packed with (Chromatographic grade Brockman activity II, BDH, Merck Ltd) alumina particles, eluted with distilled water. A mobile pale-yellow band was collected and an orange band remained adsorbed at the top of the column. The AQ27DS was recrystallized from an 80:20 acetone: water mix and the pale-yellow crystals dried in an oven at 110° C, giving a 52% yield.

High pressure liquid chromatography (HPLC) can be used to separate the isomers of anthraquinone sulphonates [21]. A sample of the (>99%) pure 2,7 isomer, prepared by a regio-selective synthesis route, was used as a standard. It was shown that the material which had been purified using the above procedure was 99.1% AQ27DS.

The ^{13}C NMR spectrum was also recorded, which showed six distinct carbon resonances, consistent with the structure of 2,7-anthraquinone disulphonate. Unpurified material showed resonances which could be attributed to other isomers.

2.2. *Electrochemical equipment*

Solutions of 1–5 mol AQ27DS m^{-3} were prepared by dissolving the appropriate mass of the sodium salt in a carbonate buffer (0.059 kmol $Na_2CO_3\,m^{-3}$, 0.223 kmol $NaHCO_3\,m^{-3}$, 0.10 kmol $Na_2SO_4\,m^{-3}$: pH 9.3) which was deoxygenated by purging with Zero Grade nitrogen (BOC plc) for two hours before use. Cyclic voltammograms were recorded using a conventional electrochemical cell with a platinum counter electrode and either a hanging mercury drop electrode (HMDE), a gold flag or a platinum foil working electrode controlled against a saturated calomel reference electrode (SCE).

A Hi-Tek PPR1 waveform generator provided programming potentials for the Wenking MP81 potentiostat, the current output from which was recorded using either a JJ Lloyd PL4 chart recorder or a Nicolet Explorer I digital storage oscilloscope.

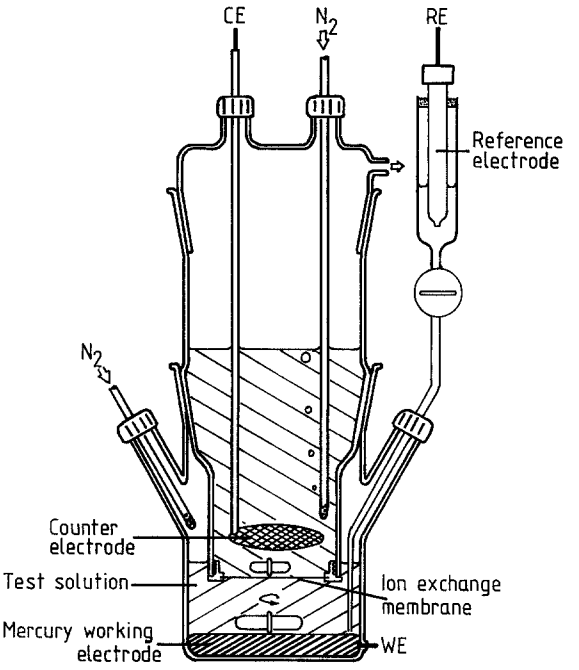

Fig. 2. Batch electrochemical reactor.

Coulometric experiments involved the cell shown in Fig. 2; this incorporated a cation exchange membrane (Nafion® 425, Du Pont Inc.) to prevent re-oxidation of the AQ27DS reduction product at the anode. The AQ27DS solution was reduced at either a titanium plate or a stirred mercury pool electrode (area $7 \times 10^{-4}\,m^2$), using a catholyte containing 3.54×10^{-4} mol dissolved in 35 cm^3 of carbonate buffer (pH 9.3). The anolyte contained 1.27×10^{-2} mol of potassium hexacyanoferrate (II) solution ($K_4Fe(CN)_6$) dissolved in the same buffer. The resulting formation of hexacyanoferrate (III) at the platinized titanium mesh anode, avoided the evolution of oxygen, which otherwise was found to diffuse through the membrane and chemically reoxidize the reduced solution in the catholyte compartment. Both compartments were deoxygenated by purging with Zero Grade nitrogen (BOC plc) prior to electrolysis, and a nitrogen atmosphere was maintained above the working solution throughout the reduction. As in all experiments reported here, the electrolyte temperature was 298 ± 2 K.

The working electrode potential was controlled using a Solartron 1286 Electrochemical Interface, and the current-time response integrated by a Hi-Tek DIBS digital integrator.

2.3. *Uv-visible spectrophotometry*

Uv-visible spectra of a Na_2AQ27DS solution was recorded at intervals throughout its reduction, whilst pumping the solution continuously through a flow-through spectrophotometer cell.

The anolyte contained 0.5 kmol m^{-3} potassium hexacyanoferrate(II) ($K_4Fe(CN)_6$) dissolved in carbonate buffer (pH 9.3) and the catholyte contained the

appropriate mass of $Na_2AQ27DS$ dissolved in the same buffer. The two solutions were separated by a Nafion® cation exchange membrane (Du Pont) and were deoxygenated by purging with oxygen-free (CP) grade nitrogen (BOC plc) before starting the reduction. A nitrogen atmosphere was maintained in the anolyte, catholyte and reference compartments throughout the experiment. The slotted titanium working electrode was maintained at -0.78 V vs SCE, which is positive of the reversible hydrogen potential at pH 9.3.

Once the solution had been deoxygenated, 3.24×10^{-4} mol of $Na_2AQ27DS$ were added to form a solution of concentration 1.392 mol m^{-3}. The initial current of -3 mA decreased with time, eventually reaching a 'residual' value of $-240\ \mu A$, which was assumed to be due to oxygen diffusion into the apparatus, causing reoxidation of the anthraquinolate product.

PTFE-lined stainless steel tubing and an enclosed diaphragm pump was used in the apparatus, to minimize effective current efficiency losses due to atmospheric oxygen diffusion into the cell. Even the short lengths of PTFE tubing, with a maximum area of 3.5×10^{-4} m^2, used to connect the inflexible metal tubing to the flow-through u.v. cell could allow enough oxygen diffusion to sustain the residual current mentioned above. Hence, a correction was made to cumulative charge measurements by subtracting the charge passed due to the experimentally observed 'residual' current.

U.v.-visible spectra were recorded at regular charge intervals using a Hewlett Packard HP8451A diode array spectrophotometer, with the solution flowing through a Hellma 170.004Q quartz cell (path length 1 mm).

2.4. *EPR spectroscopy*

The peak separation from voltammetry and the u.v.-visible spectrophotometry indicated that the radical anions, $AQ27DS^-$, were produced during the reduction of AQ27DS, even though the major product was $AQ27DSH^-$ ions. Hence, the apparatus shown in Fig. 3 was used to detect the EPR signal due to the radical anions.

Solutions of 1 and 5 mol AQ27DS m^{-3} were prepared by dissolving the appropriate mass of the sodium salt in carbonate buffer (0.059 kmol Na_2CO_3 m^{-3}, 0.223 kmol $NaHCO_3$ m^{-3}, 0.1 kmol Na_2SO_4 m^{-3}: pH 9.3). The solutions were deoxygenated by purging with nitrogen which had been purified previously by passing it through a series of Drechsel's bottles containing reduced anthraquinone-2-sulphonate (AQ2S) to remove oxygen and finally water to remove any aerosol formed. The AQ2S was reduced by contacting an alkaline solution with a zinc/mercury amalgam.

The deoxygenated solution was loaded into the drive syringe of the electrochemical EPR apparatus shown schematically in Fig. 3. A stepper motor driven syringe enabled the flow of solution through the apparatus to be carefully controlled. A potential of -0.358 V vs SHE was applied to the platinum half cylinder working electrode. The reduced solution flowed into the EPR cavity through a 1 mm diameter quartz tube, and the EPR spectrum was recorded at 9.54 GHz and 0.3395 tesla, which was swept slowly over a 5×10^{-4} tesla range, using a 0.5 s integration time constant. The integrated EPR signal strength was proportional to the magnitude of the central resonance; the cavity response was calibrated using a MgO crystal containing a known number of spins (200 p.p.m. Mn^{2+}) and measuring the resulting EPR signal.

3. Results and discussion

3.1. *Voltammetry*

Voltammograms for a hanging mercury drop electrode in aqueous alkaline solutions of AQ27DS com-

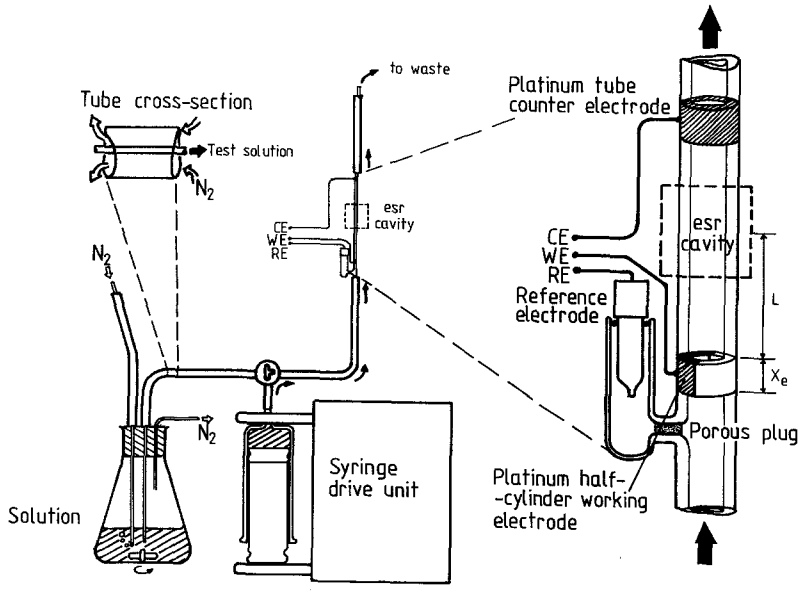

Fig. 3. Electrochemical EPR apparatus.

plied with many of the requirements of a reversible electrode reaction [22, 23]: the ratio of cathodic to anodic peak heights was unity, the potential separation $\Delta E_p = (E_p^c - E_p^a)$ of the peaks was independent of potential sweep rate (v) and the peak reduction current was proportional to the square root of v over the range 5–1000 mV s^{-1}. However, only a single reduction peak was observed, though the potential separation of the current peaks ($\Delta E_p = (E_p^c - E_p^a)$) was found to be about 40 mV (with compensation of any ohmic potential losses), precluding a simple one or two-electron reaction. Richardson and Taube [24] extended the original model [25] of the voltammetric response for two consecutive reversible one electron transfers:

$$AQ27DS + e^- \longrightarrow AQ27DS^-; \quad E_{11}^0 \quad (11)$$

$$AQ27DS^- + e^- \longrightarrow AQ27DS^{2-}; \quad E_{12}^0 \quad (12)$$

followed by fast reversible electron transfer in solution between the predominant $2e^-$ reduction product and the reactant (comproportionation):

$$AQ27DS^{2-} + AQ27DS \rightleftharpoons 2AQ27DS^- \quad (13)$$

When $E_{12}^0 - E_{11}^0 > 180$ mV, a $2e^-$ reaction response is observed with $\Delta E_p = 30$ mV between the single pair of current peaks and when $(E_{11}^0 - E_{12}^0) > 120$ mV, the two $1e^-$ reduction peaks are observed; the E^0 values can then be estimated directly from the half wave potentials. However, in the present case, the two peaks were superimposed, producing only a single reduction peak.

The peak separation ($\Delta E_p = (E_p^c - E_p^a)$) may be related [25] to the comproportionation constant (K_c):

$$K_c = \frac{[AQ27DS^-]^2}{[AQ27DS][AQ27DS^{2-}]} \quad (14a)$$

$$= \exp\{(E_{11}^0 - E_{12}^0)F/RT\} \quad (14b)$$

For example, $E_{12}^0 - E_{11}^0 = 20$ mV and 0 mV for $\Delta E_p = 37$ and 42.2 mV, respectively [21]. The observed $\Delta E_p = (E_p^c - E_p^a) \approx 40$ mV, which corresponds [21] to $(E_{11}^0 - E_{12}^0) \approx 0$. Substituting this value into Equation 14b gives $K_c \approx 1$, although the error in measuring ΔE_p is such that K_c could lie in the range 0.2 to 4.

The half wave potential of −0.25 V vs SHE at mercury, gold and platinum electrodes provided an estimate of the formal standard potential at this pH, assuming the diffusion coefficients of the oxidized (quinone) and reduced (quinolate) forms were equal. This potential was slightly more positive than the reversible potential for oxidation of HS^- ions to elemental sulphur ($E = -0.28$ V vs SHE when $[HS^-] = 10$ mol m^{-3}); the kinetics of that reaction are reported in a later paper in this series [7].

The pH dependence of the reduction potential was determined by cyclic voltammetry at a hanging mercury drop electrode, after sparging the solution with carbon dioxide for a short time, enabling the pH to be lowered from 9.3 to 7.1. Figure 4 shows a plot of the half wave potential against pH, the gradient being −31.6 mV pH^{-1}, where the Nernst equation predicts a slope of $59h/z$ mV pH^{-1} at 298 K, for a reaction involving h protons per AQ27DS molecule reduced. Hence, the predominant overall reaction in that pH range was most probably:

$$AQ27DS + H^+ + 2e^- \longrightarrow AQ27DSH^- \quad (15)$$

The peak current density at a hanging mercury drop electrode at 298 K, allowing for planar and radial diffusion of the reactant, is given by [24, 25]:

$$i_{sp} = (2.71 \times 10^5) z^{3/2} A c v^{1/2} D^{1/2} + (7.25 \times 10^4) \frac{zAcD}{r} \quad (16)$$

from which, together with the experimental peak currents, a value for D of 3.74×10^{-10} m^2 s^{-1} was calculated, assuming that $z = 2$.

Figure 5 shows cyclic voltammograms of a rotated gold disc electrode in aqueous AQ27DS solutions at

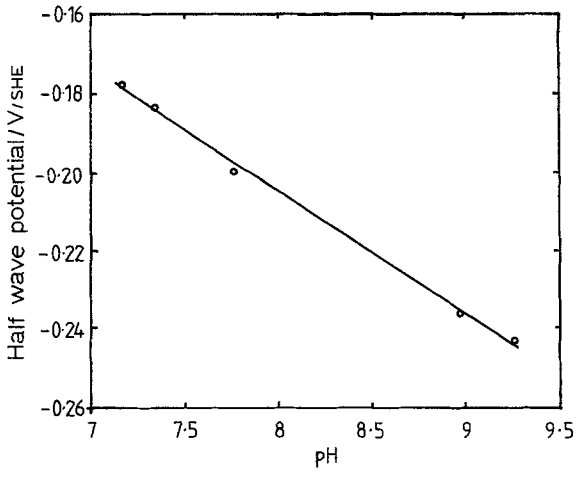

Fig. 4. pH dependence of the AQ27DS reduction potential.

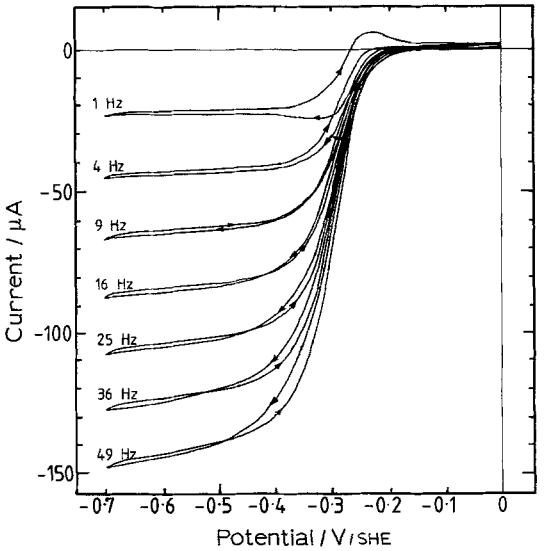

Fig. 5. Cyclic voltammetry of 0.357 mol AQ27DS m^{-3} at a rotated gold disc electrode. Potential scan rate 20 mV s^{-1}. pH 9.23.

pH 9.2; current crossovers were probably due to potential-dependent adsorption on the electrode. The currents were mass transport controlled as predicted by the Levich equation [22, 23]:

$$i_L = 1.554zFAD^{2/3}\omega^{1/2}\nu^{-1/6}c \quad (17)$$

For sequential electron transfers coupled to fast chemical reactions, the ratio of reaction layer: hydrodynamic boundary layer thicknesses is $\ll 1$ and the current response will be that of a two electron process. A plot of current against (rotation rate)$^{1/2}$ was linear, with a gradient of 2.07×10^{-5} A s$^{1/2}$, and passed though the origin. The derived diffusion coefficient (D) of 3.73×10^{-10} m^2 s^{-1}, assuming $z = 2$, was in excellent agreement with that obtained from HMDE voltammetry. For comparison, a value of 4.7×10^{-10} m^2 s^{-1} has been reported [26] for the similarly sized compound, 1,8-dihydroxyanthraquinone.

3.2. *Thermodynamic framework*

The so-called scheme of squares [for example 27] has been used to provide a framework for modelling the behaviour of sequential electron transfer reactions coupled to proton transfer. As AQ27DS is not protonated even in concentrated sulphuric acid [28], the square is incomplete:

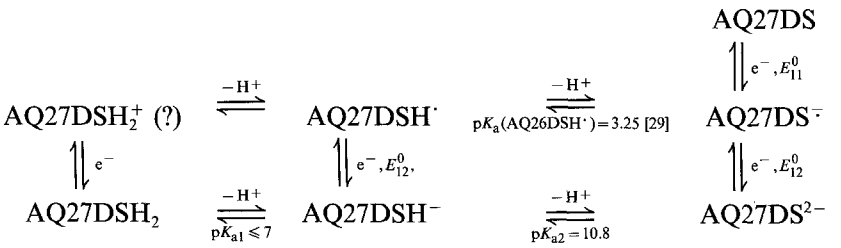

Potential–pH diagrams have been used to summarize such thermodynamic information for AQ26DS excluding radical species [30] (using pK_a(AQ26DSH$_2$) = 7.35, pK_a(AQ26DSH$^-$) = 10.35, E^0 (AQ26DS, pH 0) = 0.255 V vs SHE)), for AQ2S [31] and for *p*-benzoquinone/hydroquinone [32], for which the semiquinone intermediates are unstable to disproportionation for pH $\lesssim$ 10. Assuming that for the low concentrations used in the experimental work, concentrations can be substituted for activities in the thermodynamic equations:

$$AQ27DSH_2 \rightleftharpoons AQ27DSH^- + H^+ \quad (18)$$

$$\log\left\{\frac{[AQ27DSH^-]}{[AQ27DSH_2]}\right\} = pH - pK_{a1} \quad (19)$$

The unchanged slope of the half wave potential against pH (Fig. 5) indicates $pK_{a1} < 7.1$, though a value of 7.8 has been reported [31] and pK_{a1}(AQ26DSH$_2$) = 7.35 [30].

$$AQ27DSH^- \rightleftharpoons AQ27DS^{2-} + H^+ \quad (20)$$

$$\log\left\{\frac{[AQ27DS^{2-}]}{[AQ27DSH^-]}\right\} = pH - pK_{2a} \quad (21)$$

A value for pK_{a2} of 10.8 has been reported [31].

$$AQ27DS + 2H^+ + 2e^- \rightleftharpoons AQ27DSH_2 \quad (22)$$

$$E_{22} \text{ vs SHE/V} = (0.025 + 0.0296pK_{a1}) - 0.0591pH + 0.0296 \log\left\{\frac{[AQ27DS]}{[AQ27DSH_2]}\right\}$$

$$E_{22} \text{ vs SHE/V} \approx 0.217 - 0.0591pH + 0.0296 \log\left\{\frac{[AQ27DS]}{[AQ27DSH_2]}\right\}$$

$$AQ27DS + H^+ + 2e^- \rightleftharpoons AQ27DSH^- \quad (15)$$

$$E_{15} \text{ vs SHE/V} = 0.025 - 0.0296pH + 0.0296 \log\left\{\frac{[AQ27DS]}{[AQ27DSH^-]}\right\}$$

As analysis given above of the voltammetric behaviour at pH 9.3 indicates that the electrode potentials of the two one electron reduction reactions were fortuitously essentially equal at that pH:

$$AQ27DS + e^- \rightleftharpoons AQ27DS^{\cdot-} \quad (11)$$

$$E_{11} \text{ vs SHE/V} = -0.250 + 0.0296 \log\left\{\frac{[AQ27DS]}{[AQ27DS^{\cdot-}]}\right\}$$

$$AQ27DS^{\cdot-} + H^+ + e^- \rightleftharpoons AQ27DSH^- \quad (23)$$

$$E_{23} \text{ vs SHE/V} = 0.300 - 0.0591pH + 0.0296 \log\left\{\frac{[AQ27DS^{\cdot-}]}{[AQ27DSH^-]}\right\}$$

$$AQ27DS^{\cdot-} + e^- \rightleftharpoons AQ27DS^{2-} \quad (12)$$

$$E_{12} \text{ vs SHE/V} = -0.339 + 0.0296 \log\left\{\frac{[AQ27DS^{\cdot-}]}{[AQ27DS^{2-}]}\right\}$$

A schematic potential–pH diagram is shown in Fig. 6a, using $pK_{a2} = 10.8$ [31] and, somewhat arbitrarily, $pK_{a1} = 6.5$. Hence, the reduction mechanism is predicted to change from the predominantly comproportionation found at pH 9.3, to disproportionation at lower pH and to two one electron reductions (Reactions 11 and 12) at higher pH. However, Gamage

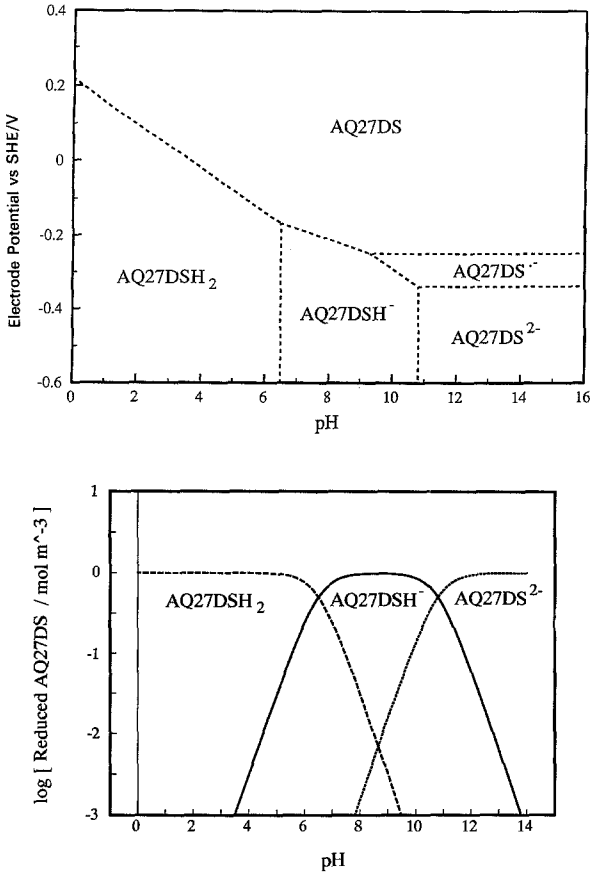

Fig. 6. (a) Schematic potential–pH diagram for AQ27DS reduction. (b) Calculated distribution of $AQ27DSH_2$, $AQ27DSH^-$ and $AQ27DS^{2-}$ species assuming pK_{a1} ($AQ27DSH_2$) = 6.5 and pK_{a2} ($AQ27DSH_2$) = 10.8 [31].

et al. [31] failed to observe separate reduction waves until they used $Et_4N^+OH^-$ as supporting electrolyte, which stabilized the $AQ27DS^{\cdot-}$ radical anions.

While useful, such diagrams show predominant species only; complementary speciation diagrams are required to explain fully the time evolution of spectra. Hence, Fig. 6b shows an activity–pH diagram for $AQ27DSH_2/AQ27DSH^-/AQ27DS^{2-}$ species *i* a composition–conversion speciation diagram is derived below, indicating that the radical anions may predominate at low conversions and/or be important minority species detectable by EPR.

3.3. *Batch reduction of AQ27DS*

The batch reduction reactor shown in Fig. 2 was calibrated using the reduction of potassium hexacyanoferrate(III) ($D_{Fe(CN)_6^{3-}} = 8.96 \times 10^{-10}\,m^2\,s^{-1}$ [33]), to obtain a mean diffusion layer thickness ($\bar{\delta}$) of 5.5 μm under the particular stirring conditions employed. Care was taken not to allow the hexacyanoferrate(III) ions to contact the mercury cathode before potential control was established, as they would otherwise have oxidized the mercury surface.

AQ27DS solutions were electrolysed at −0.382 and −0.6 V vs SHE; even the former potential was in principle sufficient to achieve a 99.99% AQ27DS conversion. Identical results were obtained at both potentials; currents decaying exponentially with time, as expected for a transport controlled reaction, and the corresponding charge rose, approaching asymptotically between 94% and 107% of the theoretical value for a two electron batch reduction. When complete reduction had been achieved, the potential of the mercury pool electrode was stepped to 0.0 V vs SHE and the solution re-oxidized with the passage of 86% of the cathodic charge.

$$AQ27DS + 2e^- \xrightarrow{\bar{k}_m} AQ27DS^{2-} \quad (24)$$

$$AQ27DS^{2-} + AQ27DS \underset{k_{-1}}{\overset{k_1}{\rightleftharpoons}} 2AQ27DS^{\cdot-} \quad (13)$$

$$K_c = \frac{k_1}{k_{-1}} = \frac{[AQ27DS^{\cdot-}]^2}{[AQ27DS][AQ27DS^{2-}]} \approx 1 \quad (14a)$$

$$K_c = \frac{k_1}{k_{-1}} = \frac{[AQ27DS^{\cdot-}]^2[H^+]}{K_{a2}[AQ27DS][AQ27DSH^-]} \approx 1 \quad (14b)$$

$$AQ27DS^{2-} + H^+ \underset{k_{-2}}{\overset{k_2}{\rightleftharpoons}} AQ27DSH^- \quad (20)$$

$$K_{a2} = \frac{k_2}{k_{-2}} = \frac{[AQ27DS^{2-}][H^+]}{[AQ27DSH^-]} \quad (21)$$

For steady state mass transport controlled reduction and provided the chemical Reactions 13 and 20 are reversible, so contributing no kinetic limitation, the usual concentration depletion equation for batch electrolysis applies:

$$[AQ27DS]_t = [AQ27DS]_0 \exp(-\bar{k}_m A t/V) \quad (25)$$

Hence, assuming 100% current efficiency, the time-dependent current density is given by:

$$\ln i_t = \ln i_{t=0} - \frac{DAt}{\bar{\delta}V} \quad (26)$$

so that the cumulative charge should then approach a value of *zFVc* coulombs asymptotically with time.

From regression on the log *i* against *t* data, the slope was determined as -1.91×10^{-4} with a correlation coefficient 0.998, from which the diffusion coefficient (*D*) of AQ27DS was estimated as $3.86 \times 10^{-10}\,m^2\,s^{-1}$, in good agreement with the values obtained from rotating disc experiments and hanging mercury drop electrode cyclic voltammetry ($3.74 \times 10^{-10}\,m^2\,s^{-1}$).

Substitution of the time-dependent AQ27DS concentration, given by Equation 25, together with Equations 14b and 20 for K_c and K_a, respectively, into the mass balance:

$$[AQ27DS]_0 = [AQ27DS]_t + [AQ27DS^{2-}] + [AQ27DSH^-] + [AQ27DS^{\cdot-}] \quad (27)$$

results in the quadratic equation for the time-dependent $AQ27DSH^-$ concentration. However, this requires prior knowledge of whether the comproportionation is Reaction 13 or, if AQ27DS reduction effectively involves concerted proton transfer by Reaction 15

to give $AQ27DSH^-$ ions, the comproportionation reaction $2e^-$ reduction product predicted to be most stable at pH 9.3.

If the protonation Reaction 20 is faster than the homogeneous electron transfer Reaction 13, the comproportionation reaction, for which the equilibrium constant was determined as approximately unity, would be:

$$AQ27DS + AQ27DSH^- \rightleftharpoons 2AQ27DS^{\cdot-} + H^+ \quad (28)$$

$$K_c = \frac{[AQ27DS^{\cdot-}]^2[H^+]}{[AQ27DS][AQ27DSH^-]} \approx 1 \quad (29)$$

This general problem, for compounds related to AQ27DS, has the subject of many papers [e.g. 9, 27, 29]. Using K_c as defined by Equation 14a results in the equation:

$$[AQ27DSH^-]^2\left\{1 + \frac{K_{a2}}{[H^+]}\right\}^2 - [AQ27DSH^-]$$
$$\left\{2[AQ27DS]_0(1 - \exp(-\bar{k}_m At/V))\left(1 + \frac{K_{a2}}{[H^+]}\right)\right.$$
$$\left. + K_c\frac{K_{a2}}{[H^+]}[AQ27DS]_0 \exp(-\bar{k}_m At/V)\right\}$$
$$+ [AQ27DS]_0^2\{(1 - \exp(-\bar{k}_m At/V))\}^2 = 0 \quad (30)$$

the solution to which, with back substitutions into Equations 14 and 21, results in the time-dependent values for $[AQ27DS^{2-}]$, $[AQ27DS^{\cdot-}]$; the corresponding values for $[AQ27DS]_t$ come from Equation 25. Typical results, plotted as a function of fractional conversion rather than time, are shown in Fig. 7 for $k_m A = 10^{-7}\,m^3\,s^{-1}$, $pK_{a2} = 10.8$ and $K_c = 1$ and pH 9.3. $AQ27DS^{\cdot-}$ radical anions are predicted to be the predominant initial product, while at long times further reduction yields $AQ27DSH^-$ and $AQ27DS^{2-}$ ions in relative concentrations determined by the pH and value of pK_{a2}; Fig. 6b shows the equilibrium distribution between the three $2e^-$ reduction products for $pK_{a1} = 6.5$ and $pK_{a2} = 10.8$ [31]. As expected, the maximum $AQ27DS^{\cdot-}$ concentration increases with the value of K_c, while larger values of pK_{a2} or lower pH increase the relative concentration of $AQ27DSH^-$ ions.

If the alternative definition of K_c, Equation 29, is used in the substitution into Equation 27, then unreasonable concentrations result. Hence, at pH 9.3 it appears that the reaction scheme involves:

$$AQ27DS + 2e^- \xrightarrow{k_m} AQ27DS^{2-}$$

$$AQ27DS^{2-} + AQ27DS \underset{k_{-1}}{\overset{k_1}{\rightleftharpoons}} 2AQ27DS^{\cdot-}$$

$$AQ27DS^{2-} + H^+ \underset{k_{-2}}{\overset{k_2}{\rightleftharpoons}} AQ27DSH^-$$

$$AQ27DSH^- + AQ27DS \underset{k_{-3}}{\overset{k_3}{\rightleftharpoons}} 2AQ27DS^{\cdot-} + H^+$$

with $k_1 \gg k_3$, though according to Equation 21, the equilibrium molar ratio of $AQ27DSH^-$ to $AQ27DS^{2-}$ is 31.6 at pH 9.3.

Such comproportionation reactions have been proposed previously for the reduction of anthraquinone in a range of solvents [34].

3.4. *U.v.-visible spectrophotometry*

The u.v.-visible spectra taken at approximately 15 C charge intervals during the reduction of AQ27DS are shown in Fig. 8, from which it can be seen that the peak at 330 nm, due to AQ27DS, decreased and two new peaks appeared as the reduction proceeded to produce a deep red solution: a sharp peak at 410 nm and a broad shoulder at 520 nm. The Beer–Lambert law was shown to be applicable over the range of

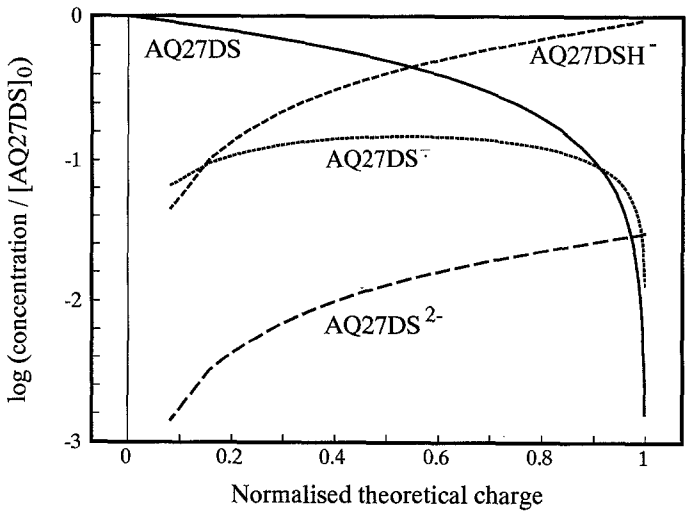

Fig. 7. Calculated distribution of AQ27DS, $AQ27DS^{\cdot-}$, $AQ27DSH^-$ and $AQ27DS^{2-}$ normalized concentrations as a function of fractional conversion during the transport controlled batch reduction of AQ27DS at pH 9.3. ($K_c = 1$ and $k_m A = 10^{-7}\,m^3\,s^{-1}$).

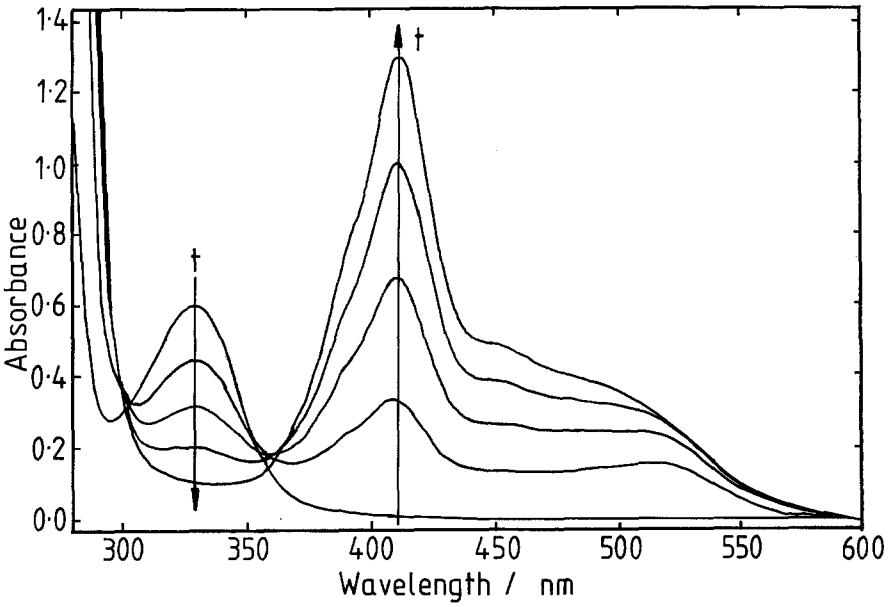

Fig. 8. Spectra taken at 15 C charge intervals during reduction of 1.392 mol AQ27DS m^{-3} at pH 9.3. Path length 1 mm.

concentrations used, enabling the absorbance at 330 nm to be used to monitor the AQ27DS concentration during its reduction; the molar absorptivity was calculated as 460.3 $m^2 mol^{-1}$.

A plot of the absorbance (330 nm) against charge (after correction for oxygen diffusion) during the reduction of AQ27DS is given in Fig. 9, which shows a linear decay as predicted, though deviations were seen as the reduction neared completion, when the charge correction due to oxygen diffusion became dominant. The charge taken to reduce the absorbance to half its initial value was 32.3 C, corresponding to 1.04 mol e^- (mol AQ27DS)$^{-1}$, suggesting the AQ27DS required 2 mol e^- (mol AQ27DS)$^{-1}$ for complete reduction, in agreement with the voltammetric behaviour.

After complete AQ27DS reduction, the spectrum showed strong peaks at 410 nm (ε = 980 $m^2 mol^{-1}$) and 277 nm ($\varepsilon \approx 10^4$ $m^2 mol^{-1}$), which were both assigned to absorptions by $AQ27DSH^-$ ions. However, the absence of an isosbestic point confirmed the presence of more than one reduction product, which is consistent with the mixture of reduction products predicted in Fig. 7.

The spectral assignments listed in Table 1 were used in the interpretation of the spectral data. The assignments originate from the work of Gamage *et al.* [31] who observed two reduction waves, corresponding to the successive one electron reactions, Reactions 11 and 12, in 0.5 kmol m^{-3} tetraethyl ammonium hydroxide at pH 13.2. Hence, by stepping to a potential intermediate between E_1 and E_2, they were able to produce and measure the spectrum of $AQ27DS^{\cdot-}$ radical anions as the predominant species, stabilized by interaction with tetraethyl ammonium cations. Kano and Matsuo [17] found that micelles of sodium laurate

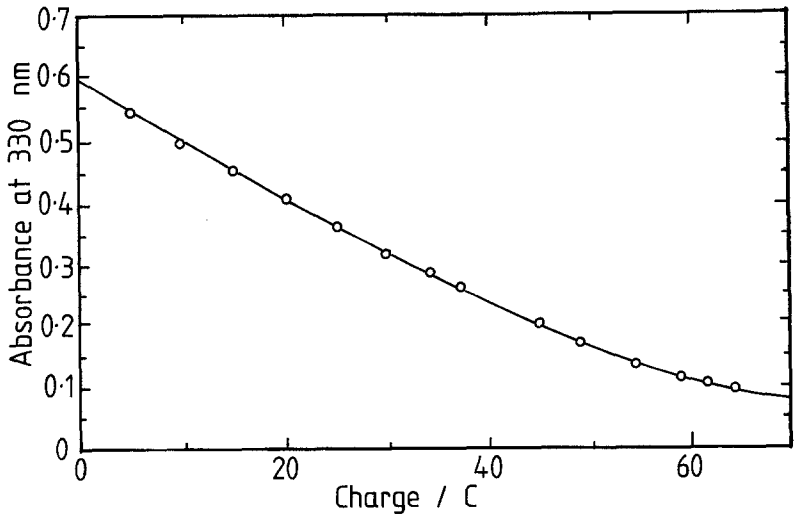

Fig. 9. Absorbance (330 nm) against charge during reduction of 1.392 mol AQ27DS m^{-3} at pH 9.3. Path length 1 mm.

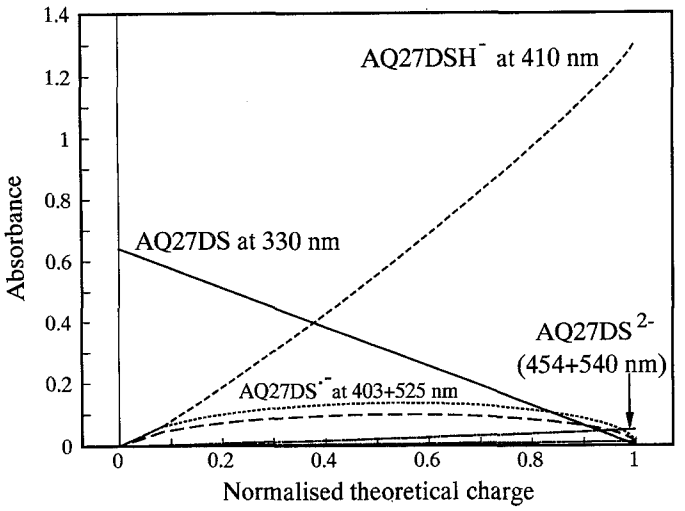

Fig. 10. Calculated absorbances due to AQ27DS, $AQ27DS^{\cdot-}$, $AQ27DSH^-$ and $AQ27DS^{2-}$ species as a function of fractional conversion, using molar absorptivities in Table 1 and concentrations from Fig. 7.

or sodium lauryl sulphate could stabilize $AQ26DS^{\cdot-}$ radical anions, but the ethyl chain used by Gamage *et al.* [31] is probably too short for micellization to occur, even at the high concentration used. Similarly, by stepping the potential to $< E_2$, they produced and measured the spectrum of $AQ27DS^{2-}$ ions. By adjusting the pH, pK_{a2} ($AQ27DSH_2$) was determined as 10.8 and further spectral assignments made for $AQ27DSH^-$ ions.

If the compositional predictions from Fig. 7 are combined with the spectral assignments in Table 1, the principal spectral changes can be predicted as a function of conversion, as shown in Fig. 10. The key changes were the disappearance of a peak at 330 nm and the appearance of a peak at 410 nm, corresponding to the depletion of AQ27DS species and accumulation of $AQ27DSH^-$ anions, respectively. The shoulder at 390 nm on the 410 nm, $AQ27DSH^-$ peak was also attributed to absorption by $AQ27DSH^-$ anions.

After the initial 15 C of charge, corresponding to 24% of the theoretical requirement for total conversion, an absorbance increase of approximately 0.1 at 525 nm is predicted by Fig. 7. This is clearly evident in the spectra shown in Fig. 8 and was due to absorption by $AQ27DS^{\cdot-}$ radical anions. A small shoulder at 454 nm in Fig. 8 also appeared at high conversions and is likely to have been due to absorption by $AQ27DS^{2-}$ ions, though according to Equation 21 present at approximately 3% of the $AQ27DSH^-$ ion concentration.

Table 1. Assignment of u.v.-visible absorbances of AQ27DS and its reduction products [31]

Species	λ_{max}/nm	ε/m^2 mol^{-1}
AQ27DS	330	460
	258	4450
$AQ27DS^{\cdot-}$	525	~660
	403	~480
$AQ27DS^{2-}$	540	~300
	454	~1200
$AQ27DSH^-$	410	~980
	277	~104

3.5. *Electrochemical EPR*

Electrochemical EPR measurements were made on solutions reduced in a flow-through tube electrode, which provided a well defined mass transport rate. Conversions were low, typically $< 2\%$, for which Fig. 7 predicts that most of the charge passed resulted in the production of radical anions at pH 9.3. The mass transport limited current for a z electron reduction at a half-cylinder electrode is given by [35]:

$$i_L = 2.75 z F X_e^{2/3} D^{2/3} V_f^{1/3} c \qquad (31)$$

where X_e is the length of electrode/m (see Fig. 3), and V_f = volumetric flow rate/m^3 s^{-1}.

A plot of i_L against $V_f^{1/3}$ was linear, with a gradient of 8.8×10^{-3} A (m^3 s^{-1})$^{-1/3}$; assuming $z = 2$, the derived value of D was 1.0×10^{-10} m^2 s^{-1}, somewhat lower than the value of 3.73×10^{-10} m^2 s^{-1} obtained using the rotating disc electrode.

Radical species produced at the tubular electrode are carried into the EPR cavity, but the velocity profile across a section of tube is parabolic. Hence, radicals produced at the tube edge diffuse towards the centre where the flow is fastest, so the number of radicals within the EPR cavity is dependent on the flow velocity profile across the tube and the rate of radial diffusion towards the centre. The resulting EPR signal strength (S) is given by [35]:

$$S = \frac{S_0(\pi/4)^{2/3} I^{2/3} r^2 i_L I'_\kappa}{z F D_0^{1/3} V_f^{2/3} I_\kappa} \qquad (32)$$

Thus the normalized signal strength (S/i_L) should be directly proportional to $V_f^{-2/3}$.

Figure 11 shows such a plot; however, EPR signal enhancement was observed at low flow rates, i.e. at

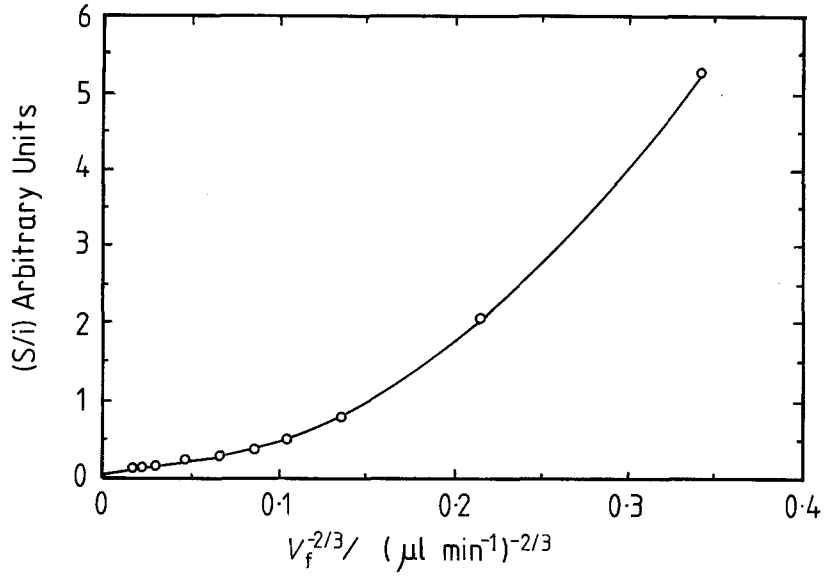

Fig. 11. Normalized EPR signal (S/i_{lim}) against $V_f^{-2/3}$.

high values of $V_f^{-2/3}$, causing deviation from linearity. This is consistent with the comproportionation mechanism of radical production. If the flow rate is slow, the reduced material undergoes greater radial diffusion, towards a region of high AQ27DS concentration, which will shift the equilibrium in Equation 14 or Reaction 28 to the right, resulting in an increased EPR signal.

Some difficulty was encountered in obtaining a fully resolved EPR spectrum; a high concentration of $AQ27DS^{\cdot-}$ increased the spin exchange owing to Equation 14 or Reaction 28, which had the effect of broadening the EPR signals, and a low concentration meant that the spectrum was hard to resolve from the instrumental 'noise'. However, using a concentration of 5 mol AQ27DS m^{-3} enabled a partially resolved EPR spectrum to be obtained which was consistent with the radical structure shown in Fig. 12 with three groups of equivalent protons, labelled H_1, H_2 and H_3. This would be expected to produce 27 resonances, but spectral overlap and line broadening would reduce this number. A spectrum was simulated using the program EPSIM77C [36] assuming the following values:

Spectral line shape	Lorentzian
Line width	0.19
Splitting constants	2.1×10^{-5} tesla (2 protons)
	5.5×10^{-5} tesla (2 protons)
	1.025×10^{-4} tesla (2 protons)

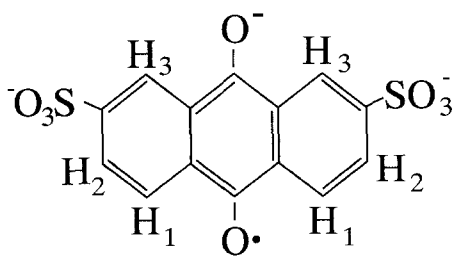

Fig. 12. Structure of $AQ27DS^{\cdot-}$.

The actual and simulated EPR spectra are shown in Fig. 13.

4. Conclusions

Anthraquinone 2,7 disulphonate (AQ27DS) was reduced in aqueous solution at pH 9.3 to give a red coloured air-sensitive solution. Cyclic voltammetry and exhaustive electrolysis indicated that the anthraquinone was reversibly reduced in a two electron, one proton process at Hg, Au and Pt electrode surfaces. The diffusion coefficient of AQ27DS was calculated to be 3.73×10^{-10} m^2 s^{-1} from mass transport controlled currents at a rotating disc electrode.

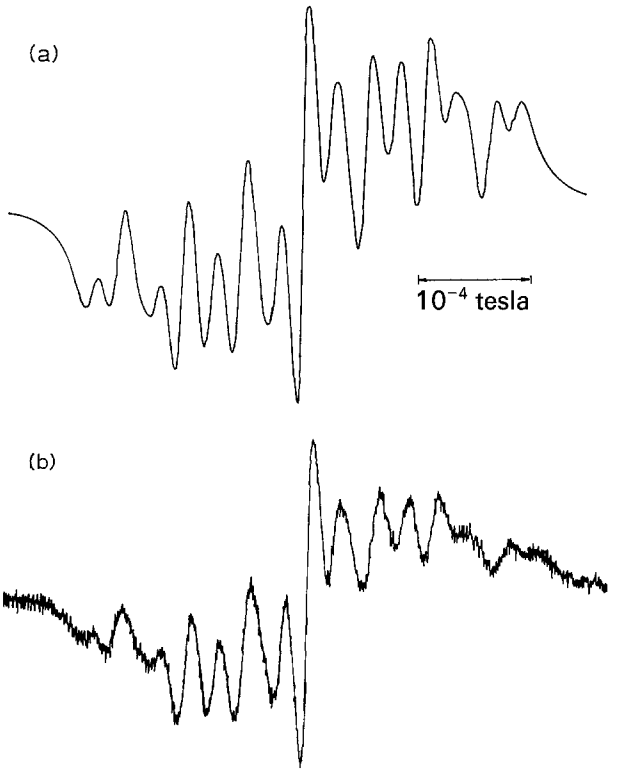

Fig. 13. (a) Simulated and (b) actual EPR spectra of $AQ27DS^{\cdot-}$.

U.v.-visible spectrophotometry confirmed that $AQ27DSH^-$ ions were the major reduced species, but also indicated that the di-anion ($AQ27DS^{2-}$) and radical species $AQ27DS^{\cdot-}$ were present in partially reduced solutions. The strong EPR signal confirmed the presence of radical species and the spectral features were consistent with the chemical structure of $AQ27DS^{\cdot-}$.

The EPR signal strength variation with flow rate showed that the radical was not produced directly at the electrode in a one electron process, but was formed via a comproportionation reaction between the di-anion and the AQ27DS starting material. The peak separation from voltammetry enabled the comproportionation constant (K_c) to be estimated as being in the range 0.2 to 4.

Acknowledgements

The authors thank the UK Science and Engineering Research Council (SERC) and British Gas for the provision of a CASE research studentship for Ian Thompson, and Dr P. Wilson for carrying out the EPR measurements. They also wish to thank Dr M. Bruce (Department of Chemistry, Manchester University) for supplying the pure 2,7 isomer which was used as a standard.

References

[1] B. M. Wilson and R. D. Newell, *Chem. Eng. Prog.* **80**(10), (1984) 40.
[2] G. H. Kelsall and I. Thompson, in Proc. Gas Research Institute (GRI) Symposium on 'Liquid Redox Processes for Hydrogen Sulphide Removal', Austin, Texas, May, 1989, GRI, Chicago (1989) pp. 34–50.
[3] I. Thompson, Ph.D. Thesis, University of London (1987).
[4] G. H. Kelsall and I. Thompson, *J. Appl. Electrochem.* **23** (1993) 279.
[5] *Idem, J. Appl. Electrochem.* **23** (1993) 287.
[6] G. H. Kelsall, I. Thompson and P. A. Francis, *J. Appl. Electrochem.* in press.
[7] G. H. Kelsall and I. Thompson, *J. Appl. Electrochem.* in press.
[8] J. Q. Chambers, 'The Chemistry of the Quinonoid Compounds', (edited by S. Patai), Wiley, New York, Pt. 2, (1974) pp. 737–93.
[9] J. Q. Chambers, 'The Chemistry of the Quinonoid Compounds', Vol. 2 (edited by S. Patai and Z. Rappoport), Wiley, New York (1988) Chap. 12, pp. 719–57.
[10] S. I. Bailey and I. M. Ritchie, *Electrochim. Acta* **30**(1), (1985) 3.
[11] G. A. Quershi, G. Svehla and M. A. Leonard, *The Analyst* **104**(1241), (1979) 705.
[12] A. Heyrovsky and B. Kuta, 'Principles of Polarography', Academic, New York (1966) 181.
[13] E. M. Savenko, D. Leibman and G. Tedoradze, *Soviet Electrochem.* **14** (1978) 404.
[14] E. M. Savenko and G. Tedoradze, *Coll. Czech. Chem. Commun.* **48** (1983) 550.
[15] J. N. Moore, Ph.D. Thesis, University of London (1986).
[16] K. Kano and T. Matsuo, *Bull. Chem. Soc. Japan.* **74** (1974) 2836.
[17] F. A. Cotton, G. Wilkinson, 'Advanced Inorganic Chemistry', 3rd. edn., Wiley Interscience, New York (1972) p. 417.
[18] B. Keita and L. Nadjo, *J. Electroanal. Chem.* **145** (1983) 431.
[19] B. Kastening and H. Schmitz, *W. German Patent 2453739* (1974).
[20] N. Ibl and H. Vogt, in 'Comprehensive Treatise on Electrochemistry', Vol 2, (edited by J. O'M. Bockris, B. E. Conway, E. Yeager, and R. E. White), Plenum Press, New York, (1981) pp. 169–208.
[21] A. Hunter, *J. Chromatography* **319** (1985) 319.
[22] E. R. Brown and J. R. Sandifer, Electrochemical Methods (Ch. 4), in 'Physical Methods of Chemistry' Vol 2, Wiley (edited by B. W. Rossiter and J. F. Hamilton) (1986) pp. 273–433.
[23] Z. Galus, Electrochemical Methods (Ch. 3), in 'Physical Methods of Chemistry', Vol 2, Wiley (edited by B. W. Rossiter and J. F. Hamilton) (1986) pp. 191–272.
[24] D. E. Richardson and H. Taube, *Inorg. Chem.* **20** (1981) 1278.
[25] D. S. Polcyn and I. Shain, *Anal. Chem.* **38**(3), (1966) 370.
[26] R. G. Compton, Ph.D. Thesis, University of Oxford (1980).
[27] E. Laviron, *J. Electroanal. Chem.* **164** (1984) 213; **169** (1984) 29.
[28] Yu. A. Kolesnik, V. V. Kozlov and L. A. Kazitsina, *Teog. Eksp. Khim.* **2**(4), (1966) 471.
[29] D. Phillips, J. N. Moore and R. E. Hester, *J. Chem. Soc., Faraday Trans. 2,* **82** (1986) 2093.
[30] O. S. Ksenzhek, S. A. Petrova, S. V. Oleinik, M. V. Kolodyazhnyi and V. Z. Moskovskii, *Soviet Electrochem.* **13**(2), (1977) 151.
[31] R. S. K. A. Gamage, A. J. McQuillan and B. M. Peake, *J. Chem. Soc., Faraday Trans.* **87** (1991) 3653.
[32] S. I. Bailey, I. M. Ritchie and F. R. Hewgill, *J. Chem. Soc., Perkin Trans.* **2** (1983) 645.
[33] D. Jahn and W. Vielstich, *J. Electrochem. Soc.* **109** (1962) 849.
[34] S. Hayano and M. Fujihira, *Bull. Chem. Soc. Japan* **44**(6), (1971) 1496.
[35] P. R. Unwin and R. G. Compton, in 'Comprehensive Chemical Kinetics', Vol. 29, Elsevier, Amsterdam (1989) pp. 297–352.
[36] C. C. Jones, Ph.D. Thesis, University of London (1984).